Carbon 116 (2017) 625–632

Contents lists available at ScienceDirect

Carbon

journal homepage: www.elsevier.com/locate/carbon

Transparency-switchable actuator based on aligned carbon nanotube and paraffin-polydimethylsiloxane composite

Wei Zhang [a, b, 1], Mingcen Weng [a, b, 1], Peidi Zhou [a, b], Luzhuo Chen [a, b, *], Zhigao Huang [a, b], Lingling Zhang [a, b], Changhong Liu [c, **], Shoushan Fan [c]

[a] Fujian Provincial Key Laboratory of Quantum Manipulation and New Energy Materials, College of Physics and Energy, Fujian Normal University, Fuzhou, 350007, China
[b] Fujian Provincial Collaborative Innovation Center for Optoelectronic Semiconductors and Efficient Devices, Xiamen, 361005, China
[c] Tsinghua-Foxconn Nanotechnology Research Center, Department of Physics, Tsinghua University, Beijing, 100084, China

ARTICLE INFO

Article history:
Received 14 November 2016
Received in revised form
6 February 2017
Accepted 17 February 2017
Available online 20 February 2017

ABSTRACT

High-performance actuators have been studied for many years, as they can be used in the fields of artificial muscles, optical switches and biomimetic applications. However, previous actuators mostly had single colors. Actuators with switchable optical properties are still rare. Here, we propose a transparency-switchable actuator based on single-layer superaligned carbon nanotube sheet and paraffin-polydimethylsiloxane composite. When a voltage is applied, the transmittance of the actuator changes from 0.7% to 67% (at the wavelength of 550 nm). At the same time, it bends obviously with a displacement up to 8.4 mm. The actuator is also durable, demonstrating both reversible actuation phenomenon and repeatable switchable transparency for 100 cycles. In addition, since this new type of actuator demonstrates optical property changing together with actuation process, which is smarter compared to previous conventional actuators, a smart window is fabricated, indicating its application in personal privacy protection and intelligent household devices. In a word, this work opens new perspectives on smart windows, optical switches and so on.

1. Introduction

Actuators can convert different types of energy, such as photonic energy, electronic energy, thermal energy and so on, into mechanical energy [1–4]. In the past decades, they have been widely used in the fields of robotics, artificial muscles, microsensors, pumps, optical devices and so on. In recent years, actuators based on carbon nanotube (CNT) and graphene have been developed rapidly and show great actuation performances [5–18]. It is worth noting that most of the carbon-based actuators were black without transparency. And there were only a few researches on carbon-based transparent actuators [18–20]. In 2013, De Hosson et al. reported an electrochromic actuator based on nanoporous metal-polymer composites [21]. However, actuators with switchable optical properties (e.g. switchable transparency) are still rare.

Materials with switchable optical properties attract great interests due to their applications in the fields of smart windows, privacy protection devices, solar controls and so on [22–30]. Switchable optical properties can be achieved under different stimulations. For example, hierarchically structured polydimethylsiloxane (PDMS) and a silica nano-particles/PDMS composite film both had switchable optical properties under mechanical stimulations [23,24]. CNT sheet and polyurethane composite could switch from opaqueness to transparency under electrical stimulation [25]. Paraffin wax (PW) and PDMS composites showed switchable transparency with external thermal stimulation [26–28]. Constructed with graphene or indium tin oxide as transparent electrodes, PW-PDMS composite could become transparent when a voltage was applied and turned back to opaque state after the voltage was turned off [29,30]. Nevertheless, the materials described above can only show switchable optical properties with stimulations. They can not show actuation performances at the

* Corresponding author. Fujian Provincial Key Laboratory of Quantum Manipulation and New Energy Materials, College of Physics and Energy, Fujian Normal University, Fuzhou, 350007, China.
** Corresponding author.
E-mail addresses: chenluzhuo@163.com (L. Chen), chliu@mail.tsinghua.edu.cn (C. Liu).
[1] These authors contributed equally.

http://dx.doi.org/10.1016/j.carbon.2017.02.053
0008-6223/

same time. There is a great need to develop a new type of high-performance actuator with switchable optical properties, which is able to show optical property changing together with actuation process. Such special type of actuator may have special applications in smart windows, optical switches and so on.

Here, we propose a new type of actuator with switchable transparency based on a layer-by-layer structure, composing of PW-PDMS composite, single-layer superaligned CNT (SACNT) sheet and polyethylene terephthalate (PET). When a direct current (DC) voltage of 120 V (2.6 V/mm) is applied, the PW-PDMS/SACNT/PET actuator becomes transparent in 20 s (with transmittance of 67% at 550 nm), and performs a bending actuation with displacement up to 8.4 mm at the same time. The actuator reverses back to opaque and straight state after the voltage is turned off. The repeatability of switchable transparency and actuation performance can be repeated for at least 100 times with no obvious degradation. Furthermore, a smart window based on the PW-PDMS/SACNT/PET actuator is proposed to verify its potential applications in privacy protection devices and other commercial products.

2. Experimental section

2.1. Materials

The single-layer SACNT sheet was obtained by directly being pulled out from the SACNT array as reported previously [31]. The PET films coated with ethylene vinyl acetate (EVA) resin were purchased from Sunwood Holding Group Co., Ltd., China. The thickness of EVA layer was 40 μm and the thickness of PET layer was 40 μm as well. The total thickness of EVA-coated PET film was 80 μm. PW with melting point of 55 °C was purchased from Shanghai Huashen Rehabilitation Equipment Factory, China. Dimethyl siloxane (DMS) and tetraethyl orthosilicate cross-link reagent were purchased from Beijing Hangtongzhou Technology Co., Ltd., China.

2.2. Fabrication of PW-PDMS/SACNT/PET composite

Fig. 1a schematically shows the layer-by-layer fabrication process of the PW-PDMS/SACNT/PET composite. Step I was the fabrication of SACNT/PET film. The single-layer SACNT sheet is in the form of aerogel [18], which is easy to be damaged. In order to maintain the transparency and conductivity of the single-layer SACNT sheet, it was firstly laid on the EVA surface of the EVA-coated PET film without strong combination. Laser was used to cut the SACNT sheet on EVA away from the continuous SACNT sheet. Secondly, after being heated at 100 °C for 5 min, the EVA was melted and the SACNTs were embedded in EVA [20]. The SACNT/PET composite film was achieved after the temperature was returned to room temperature.

Step II was adding copper electrodes. First, two ends of the SACNT/PET film were coated with silver paste. Second, the copper foils were cut into strip-shape as electrodes and two thin copper electrodes were attached to the silver paste with the aid of hand pressure [25].

Step III was the fabrication of PW-PDMS composites with 5 wt% PW. First, the DMS was mixed with PW at 80 °C to form a PW-DMS mixture, which switched from an opaque suspension to a clear gluey liquid after being stirred for 5 min. Second, the PW-DMS mixture was mixed with tetraethyl orthosilicate cross-link reagent. The weight of the cross-link reagent was the same as that of 1/9 DMS. The mixture was stirred for 10 min at 80 °C to make the cross-link reagent fully dispersed.

In the final step, the mixed liquid (PW-DMS and cross-link reagent) was directly cast onto the SACNT/PET film. The total thickness was controlled to be 1 mm by controlling the volume of mixed liquid. After curing in an oven at 65 °C for 12 h, a solid-state PW-PDMS/SACNT/PET composite was obtained. In order to show the layer-by-layer fabrication process of PW-PDMS/SACNT/PET composite more clearly, a corresponding cross-sectional schematic diagram was also shown in Fig. S1 (Supporting Information). The PW-PDMS/SACNT/PET actuator was achieved by cutting the composite with dimensions of 47 × 10 × 1 mm (length × width × thickness).

2.3. Fabrication of smart window

First, the preparation of PW-PDMS/SACNT/PET composite was the same as described above. Second, the PW-PDMS/SACNT/PET composite was cut into strip-shape with dimensions of 45 × 13 × 1 mm (length × width × thickness). The top side of the left actuator was fixed onto top frame of the window, while three sides of the right actuator were fixed onto three frames of the window. Therefore, although the right part of the smart window can not be actuated, it still has switchable transparency. Then, the smart window was achieved.

2.4. Characterization

The scanning electron microscopy (SEM) images were taken by a field emission scanning electron microscope (Hitachi SU8010). Light transmittance was measured by using a UV–Vis spectrophotometer (UV-2450, Shimadzu (China) Co., LTD.) in visible light wavelength (380 nm–800 nm). The microstructure change photos of the actuator were captured by an optical microscope (Olympus BX51M). A DC power supply (Beijing DaHua DH1722A-6) was used as the power supply to provide the DC voltage. An infrared laser distance sensor (Leuze ODSL9) was used to measure the displacement of the free end of the actuator. The temperature of the actuator was measured by a laser sight infrared thermometer (Optris LS) with temperature resolution of 0.1 °C. An infrared thermal imager (Fluke Ti10) was used to characterize the temperature distribution of the actuator. The electrical properties were measured by a digital source-meter (Keithley 2410). All optical photos were captured by a digital camera (SONY ILCE 6000).

3. Results and discussion

3.1. Design and characterization of PW-PDMS/SACNT/PET actuator

The single-layer SACNT sheet has many attractive features, such as high transparency (83%), low square resistance (~1 kΩ/square along the drawing direction) and lightweightness (1.5 μg cm^{-1}) [31,32]. It can be drawn out from the SACNT array as reported before [31]. The single-layer SACNT sheet is in the form of aerogel [18], which makes it hard to be preserved and used for further application. Therefore, the single-layer SACNT sheet is combined with the EVA-coated PET film. The role of EVA resin is to protect the SACNT sheet and fix it to the PET film, forming a transparent electrode. In such a way, the structure damage of single-layer SACNT sheet can be prevented and the high transparency together with good conductivity can be maintained. The square resistance of the SACNT/PET film is ~1 kΩ/square (along the drawing direction), as reported before [20]. Fig. 1b is a SEM image showing the surface morphology of the SACNT/PET film. Fig. S2 in Supporting Information is a SEM image with higher magnification, which verifies that the single-layer SACNT sheet is well arranged in one direction. Also, a cross-sectional SEM image of the SACNT/PET film (Fig. S3a in Supporting Information) shows that the thickness

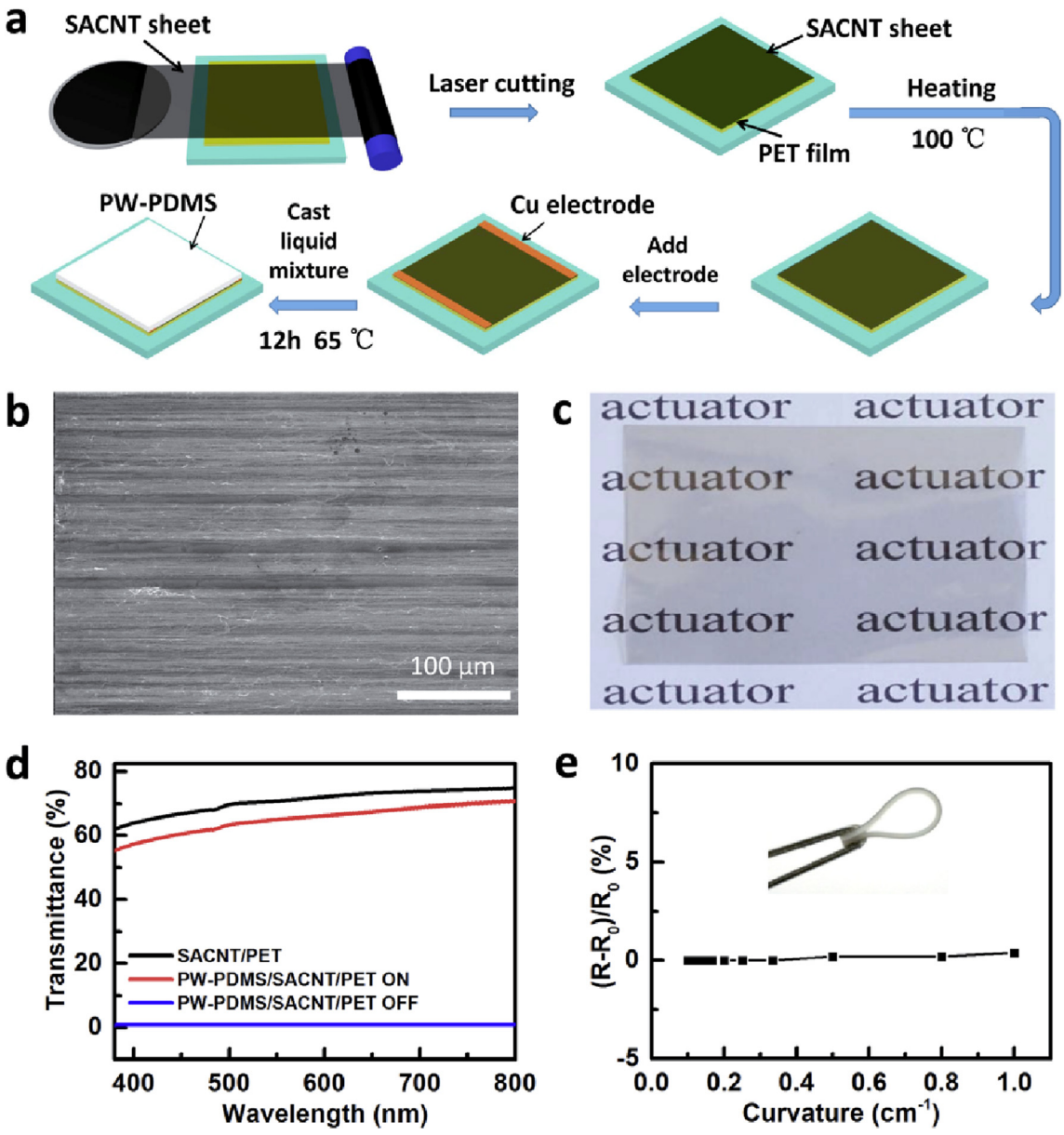

Fig. 1. (a) Schematic diagram showing the layer-by-layer fabrication process of PW-PDMS/SACNT/PET composite. (b) SEM image showing the surface morphology of SACNT/PET film. (c) Optical photo of SACNT/PET composite film showing high transparency. (d) Transmittance spectrum of SACNT/PET composite film (black line), transparent state (with voltage ON) of PW-PDMS/SACNT/PET composite (red line) and opaque state (with voltage OFF) of PW-PDMS/SACNT/PET composite (blue line). (e) The resistance change rate of the PW-PDMS/SACNT/PET composite as a function of curvature. Inset: optical photo showing the flexibility of the PW-PDMS/SACNT/PET composite. (A colour version of this figure can be viewed online.)

of SACNT-EVA layer in the SACNT/PET film is around 15 μm. Fig. S3b verifies that the SACNTs are embedded in EVA resin. Because the single-layer SACNT sheet is very thin and embedded in EVA resin, the entire thickness of the SACNT/PET film is ~80 μm, which is mostly determined by the thicknesses of the EVA-coated PET film. Fig. 1c shows that the words under the SACNT/PET film can be clearly seen by naked eyes, showing the transparency of the SACNT/PET film. The transmittance of SACNT/PET film is 72% at wavelength of 550 nm (Fig. 1d, black line).

There are three reasons for selecting these polymers to fabricate actuator with switchable transparency. First, PW can switch from opaqueness to transparency when the temperature rises above the melting point of PW. Meanwhile, PDMS is a kind of polymer with high transparency (transmittance >90% in visible light wavelength). Combined with the transparent SACNT/PET film, PW-PDMS/SACNT/PET composite is also expected to switch from opaqueness to transparency with temperature increasing. Second, the materials are flexible. The flexibility of the PW-PDMS/SACNT/PET composite is demonstrated in the insert of Fig. 1e. The *I-V* characteristics of the PW-PDMS/SACNT/PET composite clearly indicate the Ohmic characteristic of the composite, as shown in Fig. S4 (Supporting Information). The resistance change rate of the composite before and after bending is shown in Fig. 1e. The resistance of the composite increased slightly with curvature increase. When the curvature increased up to 1.0 cm^{-1}, the resistance change rate was only 0.4%. This result is in accordance with the previous report [32]. The flexibility together with nearly no conductivity change is essential for a wide range of forthcoming flexible

electronic products. Last, there are large mismatch in thermal expansion between these materials. PW has a volume expansion larger than 20% when the temperature increases from 20 °C to 120 °C [14]. PDMS has a large coefficient of thermal expansion (CTE) of 310 ppm K^{-1} [6], while the CTEs of SACNT sheet and PET film are 6 ppm K^{-1} and 38 ppm K^{-1} [6,20], respectively. Therefore, there will be great mismatch in thermal expansion between PW-PDMS composite and SACNT/PET film after the same temperature increase. Thanks to this great mismatch of CTEs, the PW-PDMS/SACNT/PET composite is expected to have a large bending deformation after being heated. These features indicate that PW-PDMS/SACNT/PET composite has great potential to be designed as an electrothermal actuator with switchable transparency and bending actuation at the same time.

3.2. Switchable transparency of PW-PDMS/SACNT/PET actuator

First of all, the optical properties of PW-PDMS/SACNT/PET actuator were studied. The actuator was totally opaque at room temperature of 23 °C, as shown in Fig. 2a. Its transmittance is below 1% (wavelength of 550 nm), as shown in Fig. 1d (blue line). The actuator can quickly switch from opaqueness to transparency under an external electrical trigger. When a DC voltage of 120 V was applied for 20 s, the actuator became transparent in 20 s, so that the word under the PW-PDMS/SACNT/PET composite can be seen by naked eyes. The transmittance was 67%, as shown in Fig. 1d (red line) as well. At the same time of transparency switching, the actuator also showed a bending actuation upward (Fig. 2b).

The switchable transparency can be explained as follows. When the temperature (23 °C) is below the melting point of PW (55 °C), the PW crystallites are solidified in PDMS matrix. Therefore, the light is scattered by PW, which results in the cloudy appearance of the PW-PDMS composite as shown in Fig. 2a. When an electrical voltage is applied, the current passes through the SACNT sheet and it is heated due to the Joule heat effect, which results in the temperature increase. Since the PW-PDMS/SACNT/PET composite is constructed by a layer-by-layer process, the PW-PDMS composite is heated in the meantime. When the temperature of the PW-PDMS composite increases above the melting point of PW, the melting of PW crystallites results in a transparent state of PW-PDMS/SACNT/PET composite, as shown in Fig. 2b. As the amount of PW is very small (5 wt%), the small amount of melting PW is still perfectly enclosed by large amount of surrounding solid-state PDMS. Hence, there will be no leakage problem.

We further studied the microstructure change of the PW-PDMS/SACNT/PET actuator with the help of an optical microscope, as

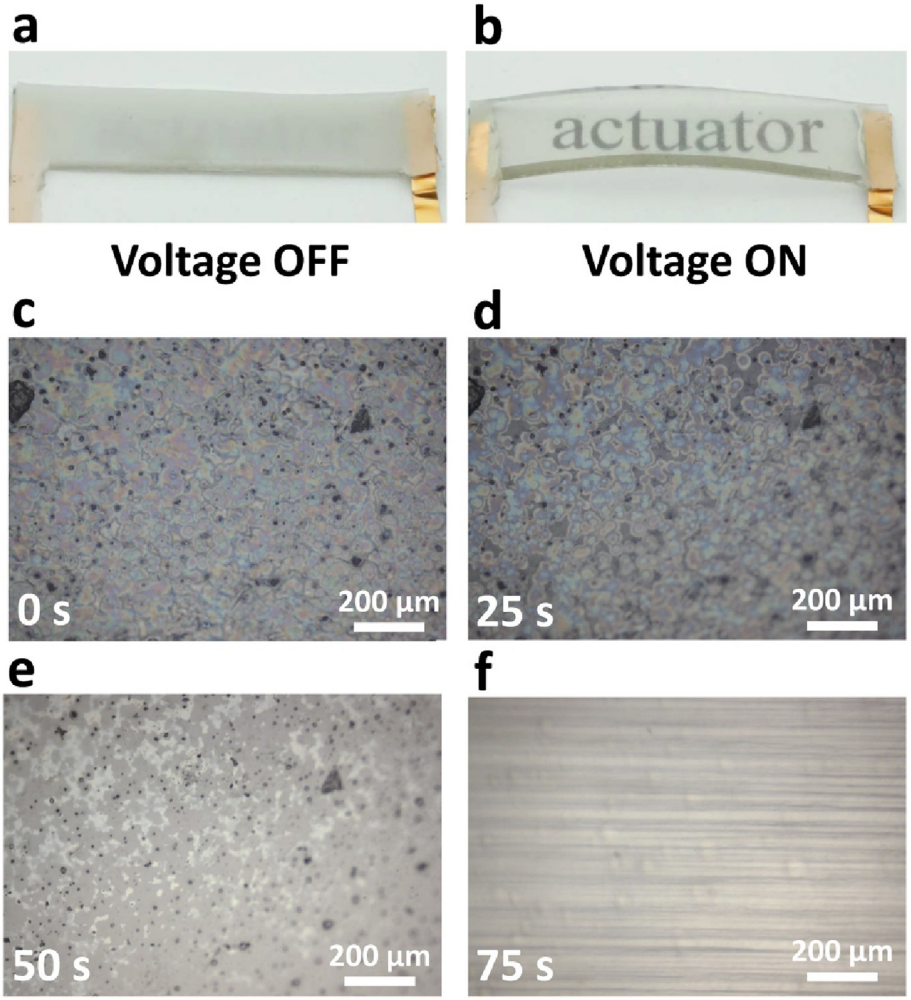

Fig. 2. (a) Optical photo of the initial opaque state of PW-PDMS/SACNT/PET actuator at room temperature (23 °C). (b) Optical photo of the transparent state of PW-PDMS/SACNT/PET actuator with a voltage of 120 V applied for 20 s (c)–(f) Microstructure change of the PW-PDMS/SACNT/PET actuator captured by the optical microscope in time sequence with a voltage of 60 V applied. (A colour version of this figure can be viewed online.)

shown in Fig. 2c–f. A DC voltage of 60 V was applied to slow down the entire optical switching process, which was easy for observation. First, PW crystallites distributed throughout the PW-PDMS composite and formed small domains (Fig. 2c). At this stage, the light which passes through the composite is scattered by dispersed PW crystallites. Therefore, the actuator showed an opaque state initially [27]. After the voltage was applied for 25 s, the temperature of the actuator increased to 39.8 °C with a portion of PW crystallites melted, as shown in Fig. 2d. After the voltage was applied for 50 s, an increasing number of PW crystallites were melted (Fig. 2e). Finally, when the temperature was higher than the melting point of PW, the PW crystallites in PW-PDMS composite were totally melted and the actuator became transparent. At this stage, the alignment structure of SACNT sheet could even be observed clearly by the optical microscope (Fig. 2f).

To further study the optical properties of the PW-PDMS/SACNT/PET actuator, different driving voltages were applied (60 V–120 V) for 60 s respectively. As shown in Fig. 3a, higher voltage resulted in a more rapid opaque-transparent switching process. It took 50 s for the actuator to become transparent with the voltage of 60 V (transmittance > 67% at 550 nm), while it took only 18 s for the actuator to become transparent with the voltage of 120 V. The response time of opaque-transparent switching was also studied, which is defined as the time to reach the transmittance of 50% at 550 nm. Fig. S5 (Supporting Information) shows the response time of PW-PDMS/SACNT/PET actuator with different driving voltages (40 V–120 V). When a low driving voltage of 40 V was applied, the response time was as long as 140 s. When a higher driving voltage of 120 V was applied, the response time quickly reduced to only 16 s. Therefore, the response time is descending with the increasing of driving voltage.

The transmittance and temperature were measured simultaneously after the PW-PDMS/SACNT/PET actuator was applied with different driving voltages (40 V–120 V) respectively for 20 s. Fig. 3b shows that the transmittance increased from 0.7% to 67% with voltage increasing. In the meantime, the temperature also increased from 30.3 °C to 74.4 °C, which was demonstrated by the infrared thermal photos in Fig. 3b. This further verifies that the switchable transparency is attributed to the temperature rise of the composite, which is caused by the Joule heat effect.

Finally, the repeatability of the opaque-transparent switching of PW-PDMS/SACNT/PET actuator was studied. The actuator was subjected to three cycles of voltage alternation. One cycle consisted of three minutes of voltage application (60 V) and two minutes of shut-off. Fig. 3c shows that the variation trend of transmittance is different from that of temperature. The temperature increased gradually with applied voltage and also decreased step by step after the voltage was shut off. The transmittance had a rapid switch when the temperature came across the melting point of PW (55 °C). When the temperature was low, the transmittance remained less than 1%. When the temperature approached the melting point of PW, the transmittance increased rapidly. The maximum transmittance was 67%. Further temperature increase had no obvious impact on the transmittance, which remained the maximum

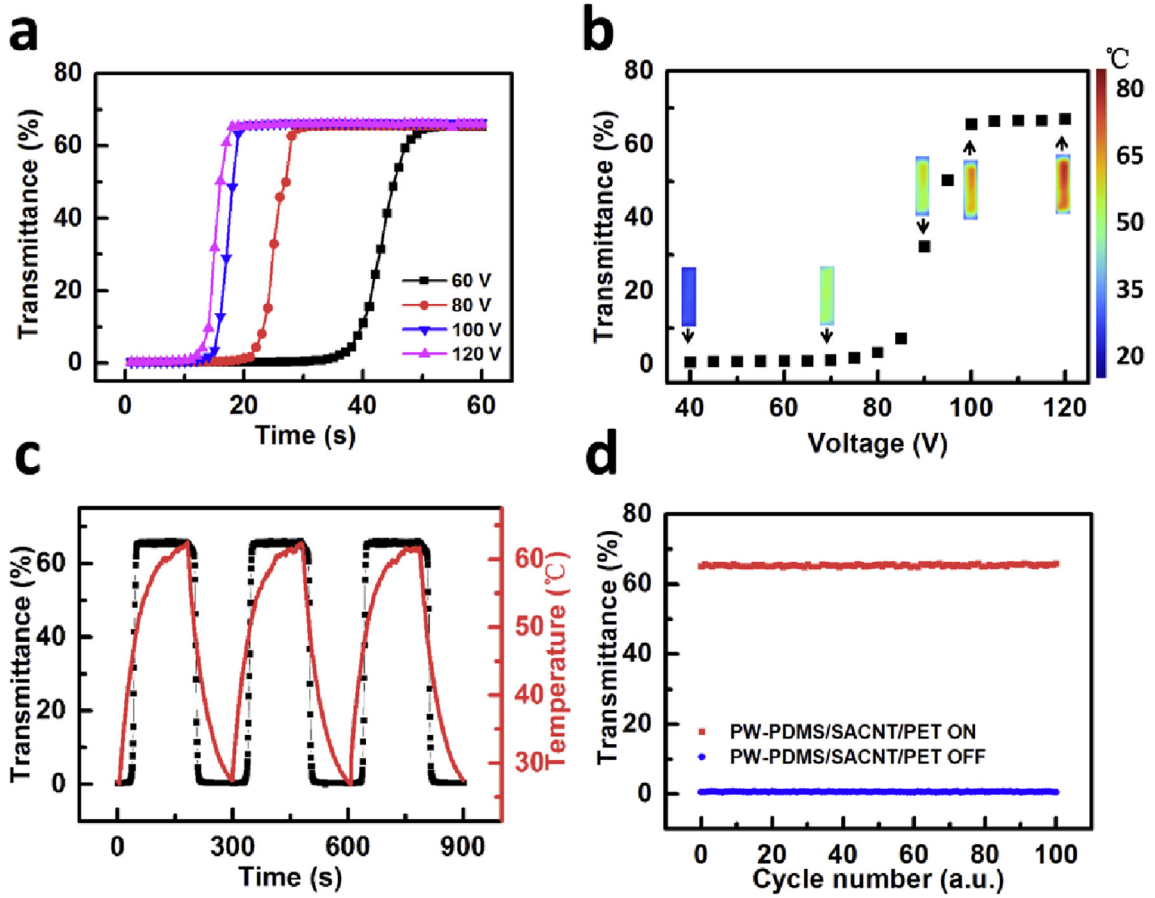

Fig. 3. (a) Transmittance (550 nm) of PW-PDMS/SACNT/PET actuator as a function of time with different driving voltages (60 V, 80 V, 100 V and 120 V). (b) Transmittance (550 nm) of the actuator as a function of driving voltage. Inset: infrared thermal photos of the actuator with different driving voltages. (c) Transmittance (550 nm) and temperature of the actuator as a function of time. (d) Repeatability test of opaque-transparent switching of the actuator. (A colour version of this figure can be viewed online.)

transmittance of 67%. On the other hand, when the temperature decreased a little, the transmittance still remained as 67%. After the temperature decreased below the melting point of PW, the transmittance quickly returned to less than 1%. Moreover, 100 times of switching cycles were further conducted. The transparent and opaque states of the PW-PDMS/SACNT/PET actuator showed no obvious change. The transmittance kept less than 1% at opaque-state (with voltage OFF), while it kept around 67% at transparent-state (with voltage ON), as shown in Fig. 3d. The transmittance and temperature of the actuator in the last three cycles were also shown in Fig. S6 (Supporting Information). It further confirms the optical switching ability after long term using.

3.3. Actuation performance of PW-PDMS/SACNT/PET actuator

It is particularly worth mentioning that the PW-PDMS/SACNT/PET actuator has not only switchable transparency, but also shows an obvious bending actuation, which has been demonstrated in Fig. 2b. Fig. 4 further illustrates the actuation performance of actuator. One end of the actuator (length of 3 mm) was fixed to a glass slide, as shown in the left panel of Fig. 4a. After a DC voltage of 120 V was applied for 20 s, the free end of the actuator bent toward the PET side with a displacement up to 8.4 mm (right panel of Fig. 4a).

As discussed in the section of "Switchable transparency of PW-PDMS/SACNT/PET actuator", when a voltage is applied, the entire actuator is heated and temperature increase results in an opaque-transparent switching. Meanwhile, the temperature increase also leads to thermal expansions of PET and PW-PDMS composite. Previous study showed that the SACNT/PET composite film exhibited no actuation with temperature change [20]. Hence, the bending actuation is mostly determined by the CTE mismatch between PW-PDMS composite and PET. Because PW-PDMS composite has a larger CTE than that of PET, the same temperature increase makes the thermal expansion of PW-PDMS composite larger than that of PET, which finally results in the bending actuation towards the PET side. This actuation mechanism is in accordance with previous studies [6,7]. After being heated, the composite film will bend to the side with a low CTE.

The displacement and temperature of the actuator were also measured simultaneously after the actuator was applied with different driving voltages (40 V–120 V). As shown in Fig. 4b, when a voltage of 40 V was applied for 20 s, the temperature increased to 30.3 °C and the displacement was only 0.6 mm. When a higher voltage of 120 V was applied for 20 s, the temperature increased up to 74.4 °C and the displacement was up to 8.4 mm. Therefore, higher temperature is obtained with higher input energy, which leads to larger actuation performance. However, if a DC voltage of 100 V was applied for 60 s, the temperature of the actuator will exceed 120 °C, resulting in damage to the actuator. Hence, when a continuous high voltage is applied and the temperature is higher than 120 °C, the actuator will break down due to long term heating.

A repeatability test of the actuation performance of PW-PDMS/SACNT/PET actuator was also conducted with a rectangular wave

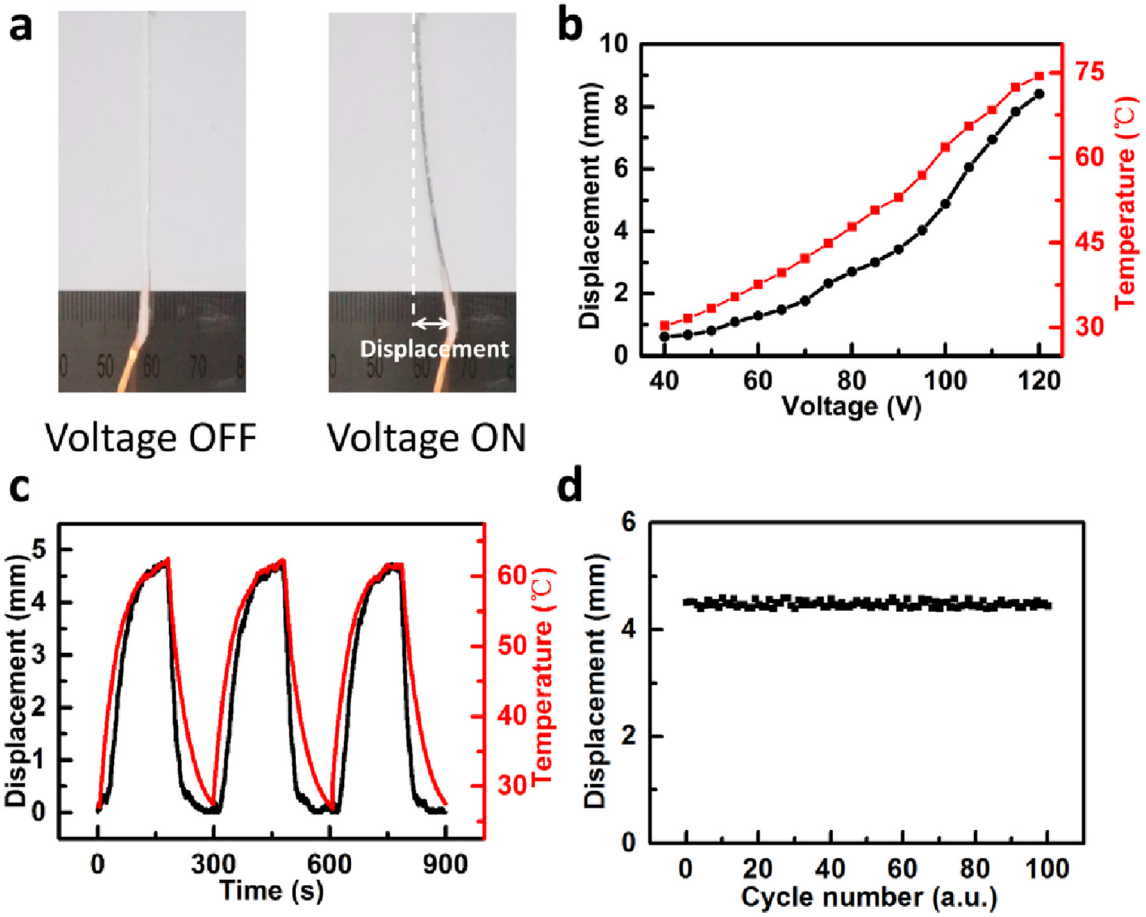

Fig. 4. (a) Optical photos of the PW-PDMS/SACNT/PET actuator without a driving voltage (left panel) and with a driving voltage of 120 V for 20 s (right panel). (b) Bending displacement and temperature of the actuator as a function of driving voltage. (c) Bending displacement and temperature of the actuator as a function of time. (d) Repeatability test of the bending performance of the actuator. (A colour version of this figure can be viewed online.)

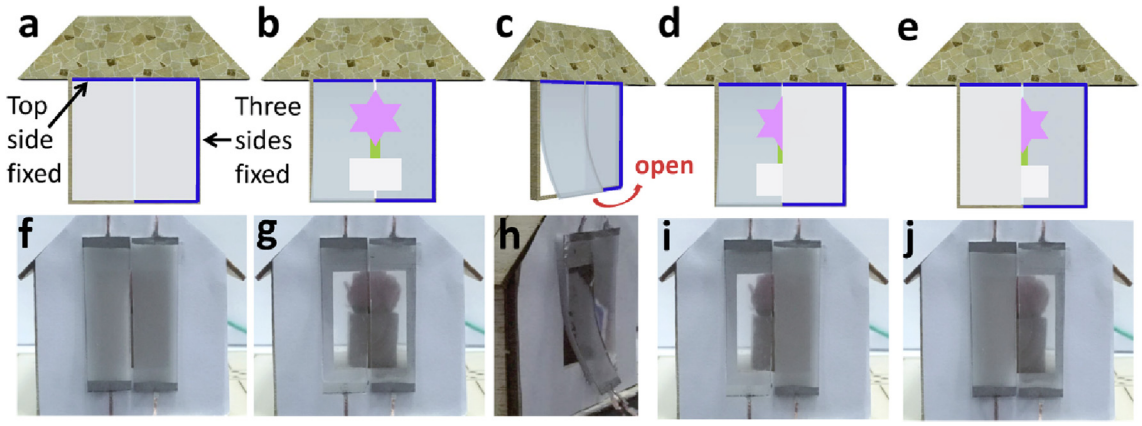

Fig. 5. (a)–(e) Schematic diagrams of smart window based on the PW-PDMS/SACNT/PET actuator. The top side of the left actuator was fixed to window frame (marked by one blue line) and the three sides of the right actuator were fixed to window frame (marked by three blue lines). (a) The initial state of smart window. (b) The smart window applied with a voltage of 120 V for 20 s (c) 45° side view of the smart window corresponding to (b). (d) The left part of the smart window applied with a voltage of 120 V for 20 s. (e) The right part of the smart window applied with a voltage of 120 V for 20 s (f)–(j) Optical photos of the smart window corresponding to (a)–(e) respectively. (A colour version of this figure can be viewed online.)

voltage (0–60 V) applied for three cycles, as shown in Fig. 4c. One cycle consisted of three minutes of voltage application (60 V) and two minutes of shut-off. The variation tendency of temperature was similar to the actuation process with the power on and off. It took the actuator 180 s to reach the maximum displacement of 4.7 mm and transmittance of 67% at the temperature of 62 °C. For the three actuation cycles, the displacement and temperature repeated well. In fact, more than 100 cycles were further conducted. As shown in Fig. 4d, the displacement was repeatable and there was no obvious degradation. In a word, Figs. 3c–d and 4c–d together show that the opaque-transparent switching and actuation performance of the PW-PDMS/SACNT/PET actuator are both repeatable, indicating the excellent stability of the actuator.

3.4. A smart window based on PW-PDMS/SACNT/PET actuator

Due to the great switchable transparency and bending actuation of the PW-PDMS/SACNT/PET actuator, we fabricated a smart window which had switchable transparency and could be opened up while an external voltage was applied. Fig. 5a–e shows the schematic diagrams of the smart window, while Fig. 5f–j shows the real working performance. As shown in Fig. 5f, two strip-shape actuators were fixed to left and right part of the window frame as described in the experimental section. In order to separately control the smart window, the actuators were in parallel connection. The switch No.1 and No. 2 were used to separately control the left part and the right part of the smart window. The circuit diagram of the smart window is shown in Fig. S7 (Supporting Information).

First, switch No. 1 and No. 2 were both turned on. Both left and right parts of the smart window were applied with a voltage of 120 V for 20 s. They both become transparent, as shown in Fig. 5b and g. Because the left part of the window had a free end, it could open at the same time, while the right part of the window was fixed with only switchable transparency (Fig. 5c and h).

Hence, this actuator with switchable transparency can be used in smart windows. Such smart window can not only change transparency, but also be opened up at the same time. As shown in Fig. 5d and i, when the switch No. 1 was turned on, only the left part of the smart window was opened up and switched from opaqueness to transparency. As described in the experimental section, three sides of right part of smart window were fixed to the window frame. Hence, on the other hand, when we only need to change the transparency of the smart window without opening it, we could turn on the switch No. 2. Then, only the right part of smart window became transparent (Fig. 5e and j).

4. Conclusions

In summary, we fabricate a new type of actuator based on PW-PDMS/SACNT/PET composite, which is able to show opaque-transparent switching and bending actuation with external electrical stimulations. With a voltage of 120 V applied for 20 s, the transmittance of the actuator increases from 0.7% to 67% at wavelength of 550 nm and the displacement of free end of the actuator is up to 8.4 mm. In addition, a smart window based on this actuator is fabricated, which can be opened up together with transparency switching. The newly designed transparency-switchable actuator is expected to show great potential in smart windows, optical switches and so on.

Acknowledgements

This work was jointly supported by National Natural Science Foundation of China (51202031, 51572146, 11504051), Natural Science Foundation of Fujian Province of China (2014J01175, 2015J01008), Fujian Provincial Program for Distinguished Young Scientists in University (J1-1166) and Fujian Provincial Key Project of Natural Science Foundation for Young Scientists in University (JZ160428).

Appendix A. Supplementary data

Supplementary data related to this article can be found at http://dx.doi.org/10.1016/j.carbon.2017.02.053.

References

[1] P. Brochu, Q. Pei, Advances in dielectric elastomers for actuators and artificial muscles, Macromol. Rapid Commun. 31 (1) (2010) 10–36.
[2] R. Shankar, T.K. Ghosh, R.J. Spontak, Dielectric elastomers as next-generation polymeric actuators, Soft Matter 3 (9) (2007) 1116–1129.
[3] K. Liu, C. Cheng, J. Suh, R. Tang-Kong, D. Fu, S. Lee, et al., Powerful, multifunctional torsional micromuscles activated by phase transition, Adv. Mater. 26 (11) (2014) 1746–1750.
[4] Y. Liu, J. Genzer, M.D. Dickey, "2D or not 2D": shape-programming polymer sheets, Prog. Polym. Sci. 52 (2016) 79–106.
[5] L.Z. Chen, C.H. Liu, C.H. Hu, S.S. Fan, Electrothermal actuation based on carbon nanotube network in silicone elastomer, Appl. Phys. Lett. 92 (26) (2008) 263104.

[6] L. Chen, C. Liu, K. Liu, C. Meng, C. Hu, J. Wang, et al., High-performance, low-voltage, and easy-operable bending actuator based on aligned carbon nanotube/polymer composites, ACS Nano 5 (3) (2011) 1588–1593.
[7] L. Chen, M. Weng, Z. Zhou, Y. Zhou, L. Zhang, J. Li, et al., Large-deformation curling actuators based on carbon nanotube composite: advanced-structure design and biomimetic application, ACS Nano 9 (12) (2015) 12189–12196.
[8] Q. Li, C. Liu, Y. Lin, L. Liu, K. Jiang, S. Fan, Large-strain, multiform movements from designable electrothermal actuators based on large highly anisotropic carbon nanotube sheets, ACS Nano 9 (1) (2015) 409–418.
[9] Y. Hu, W. Chen, L. Lu, J. Liu, C. Chang, Electromechanical actuation with controllable motion based on a single-walled carbon nanotube and natural biopolymer composite, ACS Nano 4 (6) (2010) 3498–3502.
[10] Z.H. Zeng, H. Jin, L.P. Zhang, H. Zhang, Z. Chen, F. Gao, et al., Low-voltage and high-performance electrothermal actuator based on multi-walled carbon nanotube/polymer composites, Carbon 84 (2015) 327–334.
[11] Y. Hu, T. Lan, G. Wu, Z. Zhu, W. Chen, A spongy graphene based bimorph actuator with ultra-large displacement towards biomimetic application, Nanoscale 6 (21) (2014) 12703–12709.
[12] P. Chen, Y. Xu, S. He, X. Sun, S. Pan, J. Deng, et al., Hierarchically arranged helical fibre actuators driven by solvents and vapours, Nat. Nanotechnol. 10 (12) (2015) 1077–1083.
[13] P. Chen, S. He, Y. Xu, X. Sun, H. Peng, Electromechanical actuator ribbons driven by electrically conducting spring-like fibers, Adv. Mater. 27 (34) (2015) 4982–4988.
[14] J. Deng, J. Li, P. Chen, X. Fang, X. Sun, Y. Jiang, et al., Tunable photothermal actuators based on a pre-programmed aligned nanostructure, J. Am. Chem. Soc. 138 (1) (2016) 225–230.
[15] L. Yang, K. Setyowati, A. Li, S. Gong, J. Chen, Reversible infrared actuation of carbon nanotube-liquid crystalline elastomer nanocomposites, Adv. Mater. 20 (12) (2008) 2271.
[16] J.J. Liang, L. Huang, N. Li, Y. Huang, Y.P. Wu, S.L. Fang, et al., Electromechanical actuator with controllable motion, fast response rate, and high-frequency resonance based on graphene and polydiacetylene, ACS Nano 6 (12) (2012) 11097.
[17] J. Li, W. Ma, L. Song, Z. Niu, L. Cai, Q. Zeng, et al., Superfast-response and ultrahigh-power-density electromechanical actuators based on hierarchal carbon nanotube electrodes and chitosan, Nano Lett. 11 (11) (2011) 4636–4641.
[18] A.E. Aliev, J. Oh, M.E. Kozlov, A.A. Kuznetsov, S. Fang, A.F. Fonseca, et al., Giant-stroke, superelastic carbon nanotube aerogel muscles, Science 323 (5921) (2009) 1575–1578.
[19] S. Zhu, R. Shabani, J. Rho, Y. Kim, B.H. Hong, J. Ahn, et al., Graphene-based bimorph microactuators, Nano Lett. 11 (3) (2011) 977–981.
[20] L. Chen, M. Weng, W. Zhang, Z. Zhou, Y. Zhou, D. Xia, et al., Transparent actuators and robots based on single-layer superaligned carbon nanotube sheet and polymer composites, Nanoscale 8 (12) (2016) 6877–6883.
[21] E. Detsi, P.R. Onck, J.T.M. De Hosson, Electrochromic artificial muscles based on nanoporous metal-polymer composites, Appl. Phys. Lett. 103 (19) (2013) 193101.
[22] Y. Gao, H. Luo, Z. Zhang, L. Kang, Z. Chen, J. Du, et al., Nanoceramic VO_2 thermochromic smart glass: a review on progress in solution processing, Nano Energy 1 (2) (2012) 221–246.
[23] D. Ge, E. Lee, L. Yang, Y. Cho, M. Li, D.S. Gianola, et al., A robust smart window: reversibly switching from high transparency to angle-independent structural color display, Adv. Mater. 15 (27) (2015) 2489–2495.
[24] S.G. Lee, D.Y. Lee, H.S. Lim, D.H. Lee, S. Lee, K. Cho, Switchable transparency and wetting of elastomeric smart windows, Adv. Mater. 22 (44) (2010) 5013–5017.
[25] F. Meng, X. Zhang, G. Xu, Z. Yong, H. Chen, M. Chen, et al., Carbon nanotube composite films with switchable transparency, ACS Appl. Mater. Interfaces 3 (3) (2011) 658–661.
[26] H.N. Apostoleris, M. Chiesa, M. Stefancich, Improved transparency switching in paraffin-PDMS composites, J. Mater. Chem. C 3 (6) (2015) 1371–1377.
[27] J. Zhang, G. Pu, M.R. Dubay, Y. Zhao, S.J. Severtson, Repositionable pressure-sensitive adhesive possessing thermal-stimuli switchable transparency, J. Mater. Chem. C 1 (6) (2013) 1080–1086.
[28] H. Apostoleris, M. Stefancich, S. Lilliu, M. Chiesa, Sun-tracking optical element realized using thermally activated transparency-switching material, Opt. Express 23 (15) (2015) A930.
[29] J.Y. Park, H. Song, T. Kim, J.W. Suk, T.J. Kang, D. Jung, et al., PDMS-paraffin/graphene laminated films with electrothermally switchable haze, Carbon 96 (2016) 805–811.
[30] M. Weng, L. Chen, P. Zhou, J. Li, Z. Huang, W. Zhang, Low-voltage-driven, flexible and durable paraffin–polydimethylsiloxane-based composite film with switchable transparency, Chem. Eng. J. 295 (2016) 295–300.
[31] K. Jiang, J. Wang, Q. Li, L. Liu, C. Liu, S. Fan, Superaligned carbon nanotube arrays, films, and yarns: a road to applications, Adv. Mater. 23 (9) (2011) 1154–1161.
[32] C. Feng, K. Liu, J.S. Wu, L. Liu, J.S. Cheng, Y.Y. Zhang, et al., Flexible, stretchable, transparent conducting films made from superaligned carbon nanotubes, Adv. Funct. Mater. 20 (6) (2010) 885–891.